J. Phys. B: At. Mol. Opt. Phys. 23 (1990) 1225-1234. Printed in the UK

Measurement of charge-changing cross sections in collisions of He and He^+ with H_2, O_2, CH_4, CO and CO_2

M Sataka, A Yagishita† and Y Nakai

Japan Atomic Energy Research Institute, Tokai-mura, Ibaraki 319-11, Japan

Received 13 March 1989, in final form 5 December 1989

Abstract. Single- and double-electron loss cross sections of He, and single-electron capture and single-electron loss cross sections of He^+ in collisions with H_2, O_2, CH_4, CO and CO_2 have been measured in the energy range 0.3-1.8 MeV. From the measured cross sections, charge-changing cross sections in collisions of He and He^+ with C have been determined using the Bragg rule. Scaling is examined for electron capture cross sections.

1. Introduction

Charge-changing cross sections are of importance as the basic data for many fields of application such as plasma physics and astrophysics. There are many measurements for He atoms and ions incident on atomic and molecular targets and some review articles have been published (Allison *et al* 1956, Betz 1972, Tawara and Russek 1973). So far, a number of measurements have been made for He and He^+ with the H_2 molecule as the target. For other molecules, however, the accumulation of experimental cross sections is sparse in the range above 0.3 MeV. Expansion of the measurements to higher energies is important for atomic data for fusion plasmas. Charge changing processes for He atoms and ions incident on simple molecules (H_2, O_2, CH_4, CO and CO_2) have a high priority because of the requirement for atomic and molecular data for fusion edge plasmas. Experimental study on electron capture and loss cross sections, σ_{01}, σ_{02}, σ_{10} and σ_{12}, in the energy range 0.3-1.8 MeV has been performed using a 2 MV van de Graaff accelerator. In this paper the experimental results are reported for collisions of He and He^+ with H_2, O_2, CH_4, CO and CO_2. The experimental method is described in section 2, followed by the experimental procedure and the evaluation of uncertainties in section 3.

The charge-changing cross sections for ions incident on atomic targets can be estimated using the cross sections for molecular targets by applying the Bragg rule. Toburen *et al* (1968) measured σ_{10} and σ_{01} for hydrogen projectiles incident on many molecules including carbon containing molecules in the energy range from 0.1 to 2.5 MeV. They estimated the cross sections σ_{10} and σ_{12} for H and H^+ incident on atomic carbon using the Bragg rule. For He projectiles, Itoh *et al* (1980a, b) also estimated the electron capture and loss cross sections for He, He^+ and He^{2+} incident on carbon in the energy range 0.7-2.0 MeV. Recently, Bissinger *et al* (1982) showed the additivity failure for electron capture cross sections of H^+ in the energy region

† Present address: National Laboratory for High Energy Physics, Tsukuba, Ibaraki, Japan.

0953-4075/90/071225+10$03.50

0.8–3 MeV. They explained the failure as due to intramolecular electron loss processes. Varghese *et al* (1985) measured electron capture cross sections for H^+ and He^+ in many kinds of molecular targets in the energy region 0.8–3.0 MeV and estimated σ_{10} cross sections for some atomic targets (C, O, F) by giving the correction of the intramolecular electron loss process.

In section 4, we will give the results in comparison with the measurements available at present. Electron capture and loss cross sections for He^+ and He incident on C, obtained by applying the Bragg rule to the present experimental results, will also be presented. For the single-electron capture cross section, a univeral scaling based on a combination of the Bohr–Lindhard theory and the Lenz–Jensen atomic model was proposed by Knudsen *et al* (1981). We will apply the scaling to the present results for molecules together with the earlier measurements for H_2.

2. Experimental method

Figure 1 shows a schematic diagram of the apparatus. A helium ion beam from a 2 MV van de Graaff accelerator with RF-ion source was magnetically analysed and directed into a collision chamber. The ion energy was determined within an uncertainty of ±2.5 keV. The apparatus consisted of two gas cells, two sets of electrostatic deflection plates and detectors. The gas cells were differentially pumped by three 6 in diffusion pump systems. Base pressure in the collision chamber was less than 1×10^{-7} Torr. Circular apertures a, b, c, d and e in figure 1 were machined with thin edges of 3, 1, 2, 1 and 2 mm diameter, respectively. The first gas cell, defined by apertures b and c, was used for production of the neutral beam through charge transfer from helium gas to the ion beam. The thickness of the helium gas was about 0.1 Torr cm. After passing through the first gas cell, the residual ion components were removed with the first set of deflection plates. For He ion cross sections the first gas cell was evacuated and the first deflector plates were electrically grounded. The second gas cell, defined by apertures d and e, was the target gas cell into which each target gas was introduced. The effective collision length of the target gas cell was 298 mm. The increase in the effective collision length by the gas flow from the aperture was corrected. The pressure in the target gas cell was measured with an ionisation gauge (P_5) which was frequently calibrated against a capacitance manometer (P_4). The purity of the gases was better than 99.99%. The dimensions of the apertures d and e were determined by taking the

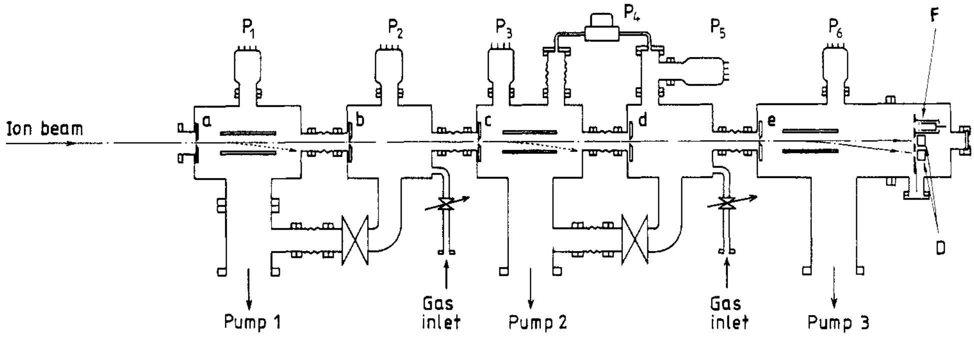

Figure 1. Schematic diagram of the apparatus.

angular distribution of the charge-changing beam and it was checked that the beam did not strike the aperture e. The neutral and charged components were measured with silicon-gold surface barrier detectors (D) with a depletion depth of 100 μm. A Faraday cup was used to measure high ion beam current.

3. Experimental procedure

The growth method (Tawara and Russek 1973) has been employed in the present study. In sufficiently thin target conditions we can easily obtain the following relation between the intensity of outgoing particles I_f, the intensity of projectiles I_i and the target pressure P at a given temperature T:

$$I_f/I_i = C + Nl\sigma_{if}P/RT \tag{1}$$

where σ_{if} is the cross section for charge changing from the charge i to the charge f; C is a constant; N is Avogadro's number; l is the effective path length of the beam in the target; P is the pressure in the target gas cell; R is the gas constant.

The quantity I_f/I_i was measured as a function of target pressure P, where I_i was obtained from the sum of the intensities of He, He^+ and He^{2+} leaving the target gas cell. As shown in equation (1), the cross section σ_{if} was determined from the slope of the linear portion in the curve of I_f/I_i against P. Values of I_i, I_f and P have been measured more than six times at a given energy. The slope of the curve has been evaluated using a least-squares fitting. The pressure region of target gases was typically less than 4×10^{-5} Torr except in the case of measurements of σ_{02} and σ_{10} at high energies.

A beam attenuation method (Gilbody *et al* 1968) was employed to check the contribution of excited species in the projectile beams of both He and He^+ to the cross sections. We tried the plot of $\log(I_f)$ against P at every measurement and obtained a linear dependence. This fact shows that the present experimental error due to the excited species is small at high energy.

The uncertainty of the cross sections came from the absolute measurement of target pressure and the determination of slope, $(I_f/I_i)/P$. The former uncertainty from the pressure measurement was estimated to be less than 5% from the repeatabilities of calibration values and the uncertainty was found to be from the least-squares fitting. Thus the present experimental errors due to the uncertainties were estimated to be less than 7% for σ_{02}, less than 10% for σ_{10} and less than 5% for σ_{01} and σ_{12}.

4. Results and discussion

The present results are listed in tables 1–4 and shown in figures 2–6.

4.1. H_2 target

Figure 2 shows the measured cross sections σ_{01}, σ_{02}, σ_{10} and σ_{12} for the H_2 target. The present results agree well within the experimental errors with the results of Allison *et al* (1956), Gilbody *et al* (1970), Hvelplund and Horsdal Pedersen (1974), Olson *et al* (1977), and Rudd *et al* (1985). The results of Pivovar *et al* (1962) agree very well with present cross sections for σ_{01} and σ_{10}. For σ_{12}, the results of Pivovar *et al* (1962) are lower than present results above approximately 1.0 MeV. The present cross sections agree fairly well with those of Itoh *et al* (1980a) for σ_{10} and those of Itoh *et*

Table 1. Single-electron loss cross sections σ_{01} (in 10^{-16} cm^2/molecule) for He incident on H_2, O_2, CH_4, CO and CO_2.

Projectile energy (MeV)	H_2	CH_4	O_2	CO	CO_2
0.3	1.14	4.95	4.35	4.29	6.21
0.4	1.27	4.77	4.37	4.52	6.56
0.5	1.16	4.68	4.38	4.58	6.75
0.6	1.07	4.37	4.39	4.67	6.67
0.7	1.04	4.40	4.35	4.59	6.66
0.8	1.01	3.96	4.16	4.41	6.35
0.9	0.927	3.56	3.95	3.97	5.83
1.0	0.876	3.36	3.72	3.64	5.53
1.2	0.769	3.20	3.47	3.35	4.99
1.4	0.734	2.98	3.24	3.06	4.75
1.6	0.571	2.73	2.99	2.75	4.35
1.8	0.512	2.56	2.83	2.61	4.14

Table 2. Double-electron loss cross sections σ_{02} (in 10^{-16} cm^2/molecule) for He incident on H_2, O_2, CH_4, CO and CO_2.

Projectile energy (MeV)	H_2	CH_4	O_2	CO	CO_2
0.3	0.0266	0.185	0.284	0.255	0.358
0.4	0.0261	0.248	0.428	0.370	0.527
0.5	0.0276	0.264	0.473	0.430	0.671
0.6	0.0314	0.269	0.493	0.466	0.710
0.7	0.0289	0.283	0.501	0.473	0.723
0.8	0.0252	0.285	0.527	0.473	0.701
0.9	0.0239	0.273	0.530	0.451	0.677
1.0	0.0226	0.253	0.521	0.427	0.661
1.2	0.0188	0.216	0.514	0.393	0.653
1.4	0.0174	0.196	0.497	0.347	0.595
1.6	0.0141	0.179	0.428	0.297	0.527
1.8	0.0118	0.161	0.392	0.275	0.480

al (1980b) for σ_{12}. The present σ_{01} data are about 40% higher than those of Itoh *et al* (1980b). The present σ_{02} data are approximately a factor of 2 smaller then those of Itoh *et al* (1980b) at 1.0 and 1.5 MeV.

Gilbody *et al* (1970) measured the electron loss cross section σ_{01} from ground-state He. Horsdal Pedersen and Hvelplund (1974) also measured cross sections σ_{01} and σ_{02} free from contribution of excited atoms to these cross sections. Since the present cross sections agree well with both sets of cross sections, the present cross sections for the neutral helium atoms may have few contribution from excited atoms.

4.2. O_2, CH_4, CO and CO_2 targets

The measured cross sections σ_{01}, σ_{02}, σ_{10} and σ_{12} for He and He^+ incident on O_2, CH_4, CO and CO_2 are shown in figures 3, 4, 5 and 6, respectively.

Table 3. Single-electron capture cross sections σ_{10} (in 10^{-16} cm^2/molecule) for He^+ incident on H_2, O_2, CH_4, CO and CO_2.

Projectile energy (MeV)	H_2	CH_4	O_2	CO	CO_2
0.3	0.501	1.75	1.30	1.32	2.24
0.4	0.264	1.04	0.927	0.861	1.23
0.5	0.139	0.566	0.590	0.530	0.820
0.6	0.0860	0.385	0.413	0.389	0.538
0.7	0.0493	0.230	0.266	0.284	0.381
0.8	0.0291	0.148	0.203	0.171	0.277
0.9	0.0214	0.103	0.155	0.121	0.207
1.0	0.0141	0.0689	0.116	0.102	0.157
1.2	0.00701	0.0371	0.0784	0.0623	0.0945
1.4	0.00392	0.0267	0.0542	0.0375	0.0613
1.6	0.00239	0.0160	0.0360	0.0275	0.0412
1.8	0.00137	0.0103	0.0269	0.0203	0.0315

Table 4. Single-electron loss cross sections σ_{12} (in 10^{-16} cm^2/molecule) for He^+ incident on H_2, O_2, CH_4, CO and CO_2.

Projectile energy (MeV)	H_2	CH_4	O_2	CO	CO_2
0.3	0.189	0.610	0.600	0.766	0.972
0.4	0.214	0.872	0.909	1.02	1.28
0.5	0.228	1.04	1.11	1.25	1.67
0.6	0.227	1.09	1.34	1.45	1.95
0.7	0.209	1.13	1.49	1.48	2.11
0.8	0.206	1.12	1.55	1.51	2.19
0.9	0.206	1.10	1.60	1.56	2.26
1.0	0.186	1.11	1.67	1.56	2.21
1.2	0.182	1.04	1.66	1.56	2.23
1.4	0.160	0.981	1.53	1.51	2.12
1.6	0.151	0.918	1.54	1.42	2.08
1.8	0.145	0.892	1.49	1.32	2.12

There have been few previous measurements in the energy region of our measurement. Barnett and Stier (1958) measured cross sections σ_{10} and σ_{12} for O_2 in the energy region less than 0.2 MeV. The present results of σ_{10} and σ_{01} for O_2 target join smoothly with their result at low energies as shown in figure 3.

Itoh *et al* (1980a) measured the cross sections σ_{10} for O_2, CH_4 and CO_2 at energy of 0.7-2.0 MeV. Itoh *et al* (1980b) also measured the cross sections σ_{01}, σ_{02} and σ_{12} for O_2, CH_4 and CO_2 at energy of 0.7-2.0 MeV. The present cross sections are about a factor of two as large as almost all the cross sections of Itoh *et al* (1980a, b) for the O_2, CH_4 and CO_2 target, except for σ_{02} and σ_{10} cross sections of the CH_4 target, as shown in figures 3, 4 and 6. This disagreement may be attributed mainly to their normalisation procedure.

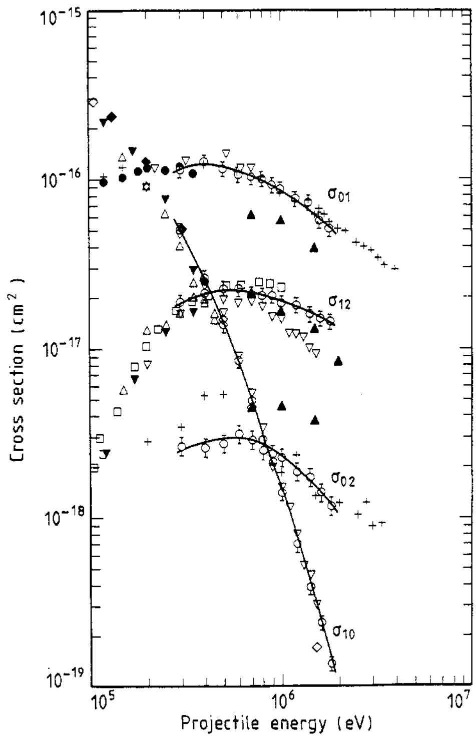

Figure 2. Single-electron loss cross sections σ_{01} and double-electron loss cross sections σ_{02} for He and single-electron capture cross sections σ_{10} and single-electron loss cross sections σ_{12} of He^+ incident on H_2: ○, σ_{01}, σ_{02}, σ_{10}, σ_{12}: present measurements; △, σ_{10}, σ_{12}: Allison *et al* (1956); ▽, σ_{01}, σ_{10}, σ_{12}: Pivovar *et al* (1962); ●, σ_{01}: Gilbody *et al* (1970); +, σ_{01}, σ_{02}: Horsdal Pedersen and Hvelplund (1974), Hvelplund and Horsdal Pedersen (1974); ◆, σ_{10}: Olson *et al* (1977); □, σ_{12}: Shah *et al* (1977); ◇, σ_{10}: Itoh *et al* (1980a); ▲, σ_{01}, σ_{02}, σ_{12}: Itoh *et al* (1980b); ▼, σ_{10}, σ_{12}: Rudd *et al* (1985).

Varghese *et al* (1985) measured cross sections σ_{10} for O_2, CH_4, CO and CO_2 at 3.2 MeV. The present results for σ_{10} join smoothly with the results of Varghese *et al* (1985) at high energy for the cross sections for O_2, CH_4, CO and CO_2 targets in figures 3, 4, 5 and 6.

Rudd *et al* (1985) measured cross sections σ_{10} and σ_{12} for O_2, CH_4, CO and CO_2 in the energy region below 0.35 MeV. The cross sections for σ_{10} and σ_{12} of O_2, CO and CO_2 agree with the present results within the experimental errors shown in figures 3, 5 and 6, but are 30–40% higher than the present results for the CH_4 target in figure 4.

4.3. C target

By using the Bragg rule, the cross sections for the carbon atom target σ_C are estimated from three kinds of combinations of $(\sigma_{CH_4} - 2\sigma_{H_2})$, $(\sigma_{CO} - \frac{1}{2}\sigma_{O_2})$ and $(\sigma_{CO_2} - \sigma_{O_2})$ with the measured cross sections. We made no corrections to the estimated cross sections by considering the intramolecular processes (Varghese *et al* 1985), because the present electron capture cross sections σ_{10} have large errors. In figure 7 the estimated cross sections, σ_{01}, σ_{02}, σ_{10} and σ_{12} for He and He^+ incident on C are shown. The average cross sections estimated from the Bragg rule are plotted with error bars to represent

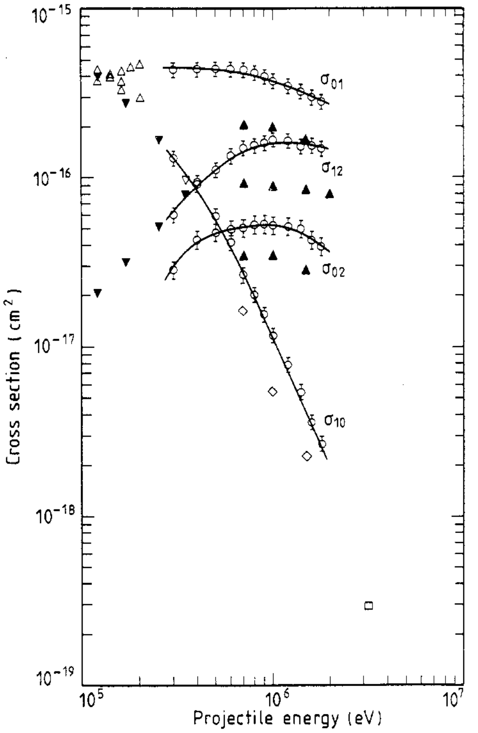

Figure 3. Single-electron loss cross sections σ_{01} and double-electron loss cross sections σ_{02} for He and single-electron capture cross sections σ_{10} and single-electron loss cross sections σ_{12} of He^+ incident on O_2: ○, σ_{01}, σ_{02}, σ_{10}, σ_{12}: present measurements; △, σ_{01}, σ_{10}: Barnett and Stier (1958); ◇, σ_{10}: Itoh *et al* (1980a); ▲, σ_{01}, σ_{02}, σ_{12}: Itoh *et al* (1980b); ▼, σ_{10}, σ_{12}: Rudd *et al* (1985); □, σ_{10}: Varghese *et al* (1985).

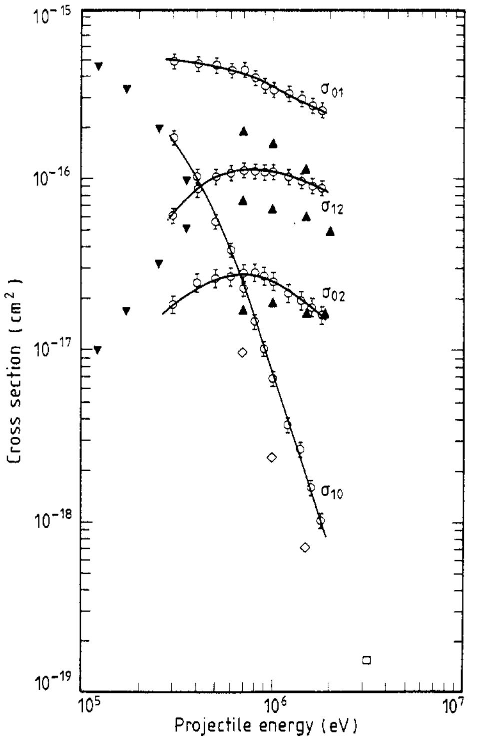

Figure 4. Single-electron loss cross sections σ_{01} and double-electron loss cross sections σ_{02} for He and single-electron capture cross sections σ_{10} and single-electron loss cross sections σ_{12} of He^+ incident on CH_4: ○, σ_{01}, σ_{02}, σ_{10}, σ_{12}: present measurements; ◇, σ_{10}: Itoh *et al* (1980a); ▲, σ_{01}, σ_{02}, σ_{12}: Itoh *et al* (1980b); ▼, σ_{10}, σ_{12}: Rudd *et al* (1985); □, σ_{10}: Varghese *et al* (1985).

the maximum deviation of calculated cross sections from the average cross sections. The maximum deviations from the average cross sections are less than 30% for σ_{01}, σ_{02} and σ_{12}. The maximum deviations for σ_{10} are less than 55%, due to the large uncertainty of the measured σ_{10} cross section. As the average cross sections vary smoothly as a function of incident energy, the Bragg rule can be applicable to estimate the atomic cross sections for helium even in the energy region less than a few MeV. The cross sections estimated by Varghese *et al* (1985) lie on an extrapolation along the present values to higher energy. The values of Itoh *et al* (1980a, b) are a factor of 4–12 smaller than the present values. The difference may result from underestimating their cross sections for carbon-containing molecules.

4.4. Comparison between σ_{10} cross sections for He^+ ions

Knudsen *et al* (1981) derived a universal scaling for σ_{10} of highly charged ions in collisions of atoms, that is, the reduced cross sections $\sigma_{10}Z^{2/3}/\pi a_0^2 q$ depend on the value of $E(\mathrm{keV\,amu^{-1}})q^{-4/7}Z^{-16/21}$ only. Here Z is the target atomic number, a_0 the Bohr radius, q the charge of ion, and E the ion energy. In order to apply the scaling

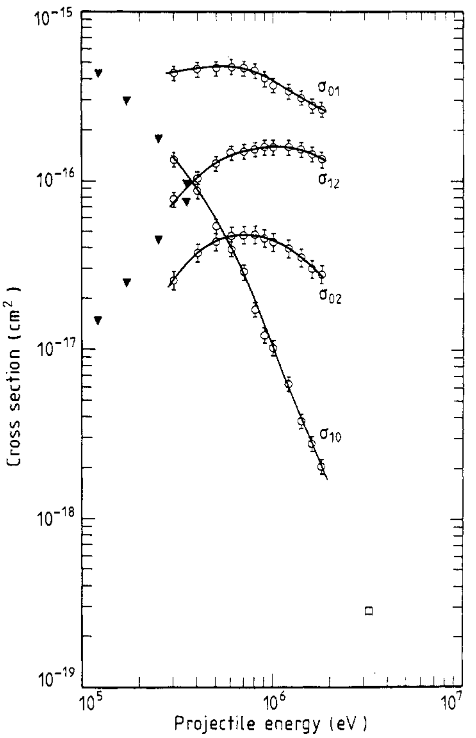

Figure 5. Single-electron loss cross sections σ_{01} and double-electron loss cross sections σ_{02} for He and single-electron capture cross sections σ_{10} and single-electron loss cross sections σ_{12} of He^+ incident on CO: ○, σ_{01}, σ_{02}, σ_{10}, σ_{12}: present measurements; ▼, σ_{10}, σ_{12}: Rudd *et al* (1985); □, σ_{10}: Varghese *et al* (1985).

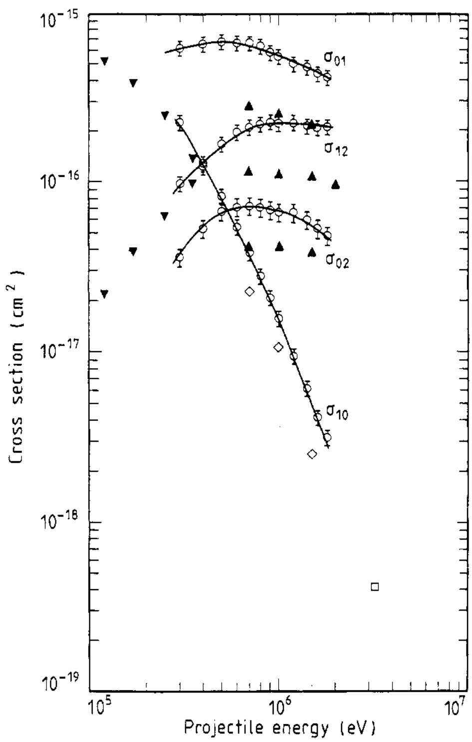

Figure 6. Single-electron loss cross sections σ_{01} and double-electron loss cross sections σ_{02} for He and single-electron capture cross sections σ_{10} and single-electron loss cross sections σ_{12} of He^+ incident on CO_2: ○, σ_{01}, σ_{02}, σ_{10}, σ_{12}: present measurements; ◇, σ_{10}: Itoh *et al* (1980a); ▲, σ_{01}, σ_{02}, σ_{12}: Itoh *et al* (1980b); ▼, σ_{10}, σ_{12}: Rudd *et al* (1985); □, σ_{10}: Varghese *et al* (1985).

to the present results for molecules, we use an effective Z defined by Henriksen and Baarli (1957) using Bragg's additive rule, $Z^k = \Sigma_i Z_i^k$ for scaling of σ_{10} with $k = \frac{2}{3}$ and of E with $k = -\frac{16}{21}$, where Z_i is the atomic number of an atom of a molecule.

Figure 8 shows the results of the scaling applied to the present results, in comparison with the earlier measurements. Although the scaling proposed by Knudsen *et al* (1981) is applicable for $q > 4$, it is seen that σ_{10} for O_2, CO, CO_2 and CH_4 molecules are scaled well on a single curve. However, the scaling does not work well in the case of the H_2 molecule. This may be because the statistical Lenz-Jensen atomic model Knudsen *et al* (1981) employed does not hold good for the H_2 molecule.

Acknowledgment

The authors would like to acknowledge to Dr C F Barnett of Oak Ridge National Laboratory for valuable discussions and a critical reading of the manuscript. Dr T Shirai was most helpful with useful discussions and encouragement throughout this

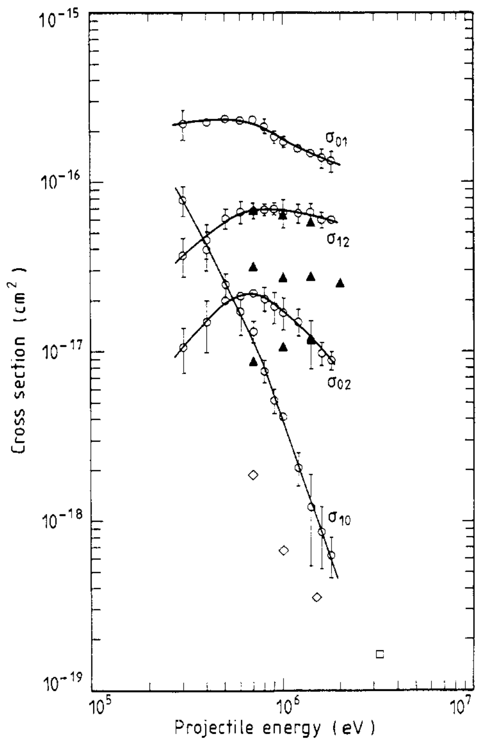

Figure 7. Single-electron loss cross sections σ_{01} and double-electron loss cross sections σ_{02} for He and single-electron capture cross sections σ_{10} and single-electron loss cross sections σ_{12} of He^+ incident on carbon atom; ○, σ_{01}, σ_{02}, σ_{10}, σ_{12}: present results; ◇, σ_{10}: Itoh *et al* (1980a); ▲, σ_{01}, σ_{02}, σ_{12}: Itoh *et al* (1980b); □, σ_{10}: Varghese *et al* (1985).

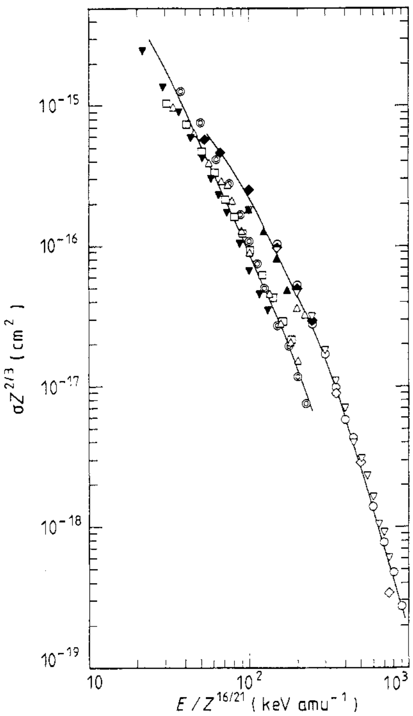

Figure 8. A comparison between electron capture cross sections σ_{10} for He^+ incident on H_2, O_2, CH_4, CO, CO_2 molecules: ○, H_2: present results; ▲, H_2: Allison *et al* (1956); ▽, H_2: Pivovar *et al* (1962); ◆, H_2: Olson *et al* (1977); ◇, H_2: Itoh *et al* (1980a); ◎, CH_4: present results; □, O_2: present results; △, CO: present results; ▼, CO_2: present results.

experiment. The authors also gratefully acknowledge Dr K Ozawa for providing valuable consultation on the experiment.

References

Allison S K, Cuevas J and Murphy P G 1956 *Phys. Rev.* **102** 1041
Barnett C F and Stier P M 1958 *Phys. Rev.* **109** 385
Betz H D 1972 *Rev. Mod. Phys.* **44** 465
Bissinger G, Joyce J M, Lapicki G, Laubert R and Varghese S L 1982 *Phys. Rev. Lett.* **49** 318
Gilbody H B, Browning R, Levy G, McIntosh A I and Dunn K F 1968 *J. Phys. B: At. Mol. Phys.* **1** 863
Gilbody H B, Dunn K F, Browning R and Latimer C J 1970 *J. Phys. B: At. Mol. Phys.* **3** 1105
Henriksen T and Baarli J 1957 *Radiat. Res.* **6** 415
Horsdal Pedersen E and Hvelplund P 1974 *J. Phys. B: At. Mol. Phys.* **7** 132
Hvelplund P and Horsdal Pedersen E 1974 *Phys. Rev.* A **9** 2434
Itoh A, Asari M and Fukuzawa F 1980a *J. Phys. Soc. Japan* **48** 943
Itoh A, Ohnishi K and Fukuzawa F 1980b *J. Phys. Soc. Japan* **49** 1513
Knudsen H, Haugen H K and Hvelplund P 1981 *Phys. Rev.* A **23** 597
Olson R E, Salop A, Phaneuf R A and Meyer F W 1977 *Phys. Rev.* A **16** 1867

Pivovar L I, Tubaev V M and Novikov M T 1962 *Sov-Phys.-JETP* **14** 20
Rudd M E, Goffe T V, Itoh A and DuBois R D 1985 *Phys. Rev.* A **32** 829
Shah M B, Goffe T V and Gilbody H B 1977 *J. Phys. B: At. Mol. Phys.* **10** L723
Tawara H and Russek A 1973 *Rev. Mod. Phys.* **45** 178
Toburen L H, Nakai M Y and Langley R A 1968 *Phys. Rev.* **171** 114
Varghese S L, Bissinger G, Joyce J M and Laubert R 1985 *Phys. Rev.* A **31** 2202